Refractory, Ceramic, and Composite Materials
Тугоплавкие, керамические и композиционные материалы

**UDC** 661.66
https://doi.org/10.17073/1997-308X-2025-1-30-39

***Research article***
***Научная статья***

# Crystalline structure of polyacrylonitrile- and viscose-based carbon fibers following high-temperature treatment in the range of 1500–2800 °C

**B. S. Kleusov[1], V. M. Samoilov[1], V. A. Elchaninova[1], D. A. Budushin[1], E. M. Litovchenko[2], A. S. Poplavskaya[1], V. A. Vorontsov[1]**

[1] **JSC "Scientific Research Institute of Structural Materials based on graphite named after S.E. Vyatkin"**
1 Bld, 2 Electrodnaya Str., Moscow 111524, Russia
[2] **D.I. Mendeleev Russian University of Chemical Technology**
1 Bld, 20 Geroev Panfilovtsev Str., Moscow 125480, Russia

BSKleusov@rosatom.ru

***Abstract.*** The crystalline structure of carbon fibers (CF) based on polyacrylonitrile (PAN) and viscose precursors, treated in the temperature range of 1500 to 2800 °C, was studied using *X*-ray diffraction analysis and Raman spectroscopy. The objective of the study was to obtain data on the structure of low-modulus viscose-based fibers, which are widely used as fillers in composite materials, and to compare the characteristics of CF derived from different precursors. An empirical dependence of the intensity ratio of the *D* and *G* lines ($I_D/I_G$) of the Raman spectra on the treatment temperature was established for carbon fibers based on viscose and PAN. The crystallite sizes $L_a$ and $L_c$ of both types of CF obtained at different treatment temperatures were evaluated. It was revealed that as the treatment temperature increases, the crystallite sizes $L_a$ and $L_c$ grow, while the interlayer spacing $d_{002}$ decreases, indicating an increase in the degree of graphitization. It was found that viscose-based carbon fibers exhibit a less ordered crystalline structure compared to PAN fibers processed under the same conditions. Additionally, the true density and elastic modulus of viscose-based CF were investigated, showing lower values than those of PAN fibers treated at the same temperature. These differences in the properties and structure of CF are attributed to the microtextured nature of viscose fibers. However, during treatment at 2800 °C, CF undergo partial graphitization, which significantly reduces structural differences between fibers of both types. Nevertheless, despite the similarity in crystalline structure, viscose-based CF, even after high-temperature treatment, does not become analogous to PAN-based fibers.

***Keywords:*** carbon fibers, *X*-ray phase analysis, Raman spectroscopy

***For citation:*** Kleusov B.S., Samoilov V.M., Elchaninova V.A., Budushin D.A., Litovchenko E.M., Poplavskaya A.S., Vorontsov V.A. Crystalline structure of polyacrylonitrile- and viscose-based carbon fibers following high-temperature treatment in the range of 1500–2800 °C. *Powder Metallurgy and Functional Coatings*. 2025;19(1):30–39.
https://doi.org/10.17073/1997-308X-2025-1-30-39

# Кристаллическая структура углеродных волокон на основе полиакрилонитрила и вискозы после высокотемпературной обработки в интервале температур 1500–2800 °C

**Б. С. Клеусов[1], В. М. Самойлов[1], В. А. Ельчанинова[1], Д. А. Будушин[1], Е. М. Литовченко[2], А. С. Поплавская[1], В. А. Воронцов[1]**

[1] **АО «Научно-исследовательский институт конструкционных материалов на основе графита» им. С.Е. Вяткина**
Россия, 111524, г. Москва, ул. Электродная, 2, стр. 1
[2] **Российский химико-технологический университет им. Д.И. Менделеева**
Россия, 125480, г. Москва, ул. Героев Панфиловцев, 20, корп. 1, стр. 2

BSKleusov@rosatom.ru

***Аннотация.*** Методами рентгеновского дифракционного анализа и спектроскопии комбинационного рассеяния проведено исследование кристаллической структуры углеродных волокон (УВ) на основе полиакрилонитрила (ПАН) и вискозы, обработанных в диапазоне температур от 1500 до 2800 °C. Целью исследования было получение данных о структуре низкомодульных волокон на основе вискозы, имеющих широкое применение в качестве наполнителей композиционных материалов, а также сравнение характеристик УВ на основе разных прекурсоров. Получена эмпирическая зависимость отношения интенсивностей линий *D* и *G* ($I_D/I_G$) спектров комбинационного рассеяния от температуры обработки для углеродных волокон на основе вискозы и ПАН. Проведена оценка размеров кристаллитов ($L_a$ и $L_c$) обоих типов УВ, полученных при различных температурах обработки. Выявлено, что с ростом температуры обработки волокон происходит увеличение размеров кристаллитов $L_a$ и $L_c$, а межслоевое расстояние ($d_{002}$) уменьшается, что указывает на повышение степени графитации. Установлено, что углеродные волокна на основе вискозы имеют менее совершенную кристаллическую структуру по сравнению с ПАН-волокнами, обработанными в тех же условиях. Также были исследованы истинная плотность и модуль упругости УВ на основе вискозы, у которых оказались более низкие значения, чем у ПАН-волокон с той же температурой обработки. Данные различия в свойствах и структуре УВ обусловлены микротекстурированностью вискозного волокна. Однако в процессе обработки при температуре 2800 °C УВ претерпевают частичную графитацию, что в значительной степени нивелирует структурные различия между волокнами обоих видов. Тем не менее, несмотря на сходство кристаллической структуры, УВ на основе вискозы даже после высокотемпературной обработки не становятся аналогом ПАН-волокна.

***Ключевые слова:*** углеродные волокна, рентгенофазовый анализ, рамановская спектроскопия

***Для цитирования:*** Клеусов Б.С., Самойлов В.М., Ельчанинова В.А., Будушин Д.А., Литовченко Е.М., Поплавская А.С., Воронцов В.А. Кристаллическая структура углеродных волокон на основе полиакрилонитрила и вискозы после высокотемпературной обработки в интервале температур 1500–2800 °C. *Известия вузов. Порошковая металлургия и функциональные покрытия*. 2025;19(1):30–39. https://doi.org/10.17073/1997-308X-2025-1-30-39

## Introduction

The development of carbon fiber-reinforced plastics has led to the production of a wide range of carbon fibers (CF) [1–6]. The existing classification divides all CF into several types based on their modulus: low-modulus (30–100 GPa), intermediate-modulus and high-strength (200–350 GPa), high-modulus (350–500 GPa), and ultra-high-modulus (500–1000 GPa) [6–11]. Another critical factor in classifying fibers is the precursor type, which determines the crystalline structure of CF and, ultimately, its final properties [6–11]. Currently, nearly all commercially produced CF are derived from three main precursors: polyacrylonitrile (PAN), isotropic and mesophase pitches, and viscose [6–11].

The crystalline structure of PAN- and mesophase pitch-based CF has been extensively studied using *X*-ray diffraction, often in combination with Raman spectroscopy and electron microscopy [12–17]. However, the structure of viscose-based fibers remains underexplored. Existing data in early literature [18; 19] pertain to the technology for producing intermediate- and high-modulus viscose-based CF, developed over 50 years ago in the United States. Studies on the crystalline structure of low-modulus (30–100 GPa) viscose-based CF are extremely limited [20–22], despite their widespread use as fillers in composite materials for various applications.

The aim of this study was to investigate the crystalline structure of viscose-based carbon fibers and its

changes during high-temperature treatment, with a comparative analysis of similar data for PAN-based CF.

## Materials and methods

For this study, semi-finished products of TGN-brand viscose-based CFs and UKN-type PAN-based CFs, both manufactured in the Russian Federation, were used. The samples were obtained by additional heat treatment (HT) of CF bundles in a laboratory Tammann furnace under argon atmosphere in a free state (without tension). The heating rate was 300 °C/h, and the dwell time at the target temperature was 20 min. The processing temperature was monitored using a pyrometer.

The true density of the obtained CF samples was measured using the gradient tube method in accordance with GOST R ISO 10119–2012. The average filament diameter, tensile strength, and dynamic elastic modulus of single filaments were measured according to ASTM D4018–11. The physical and mechanical properties of CF were determined as averages from 25 measurements of tensile strength and elastic modulus, following GOST 6943.5–79 and GOST 28008–88.

Raman spectra of CF subjected to various HT temperatures ($t_{HT}$) were recorded from the lateral surface of filaments in the broad spectral range of 700–3000 $cm^{-1}$ using a confocal Raman microspectrometer Via Reflex (Renishaw, UK) equipped with an optical microscope and a cooled CCD detector. The laser spot size at 100× magnification was 0.5 μm. The excitation source was a diode-pumped solid-state Nd:YAG laser with a wavelength of 532 nm and a power of 1 mW.

In the first-order spectrum (1000–2000 $cm^{-1}$), carbon materials, including CF, typically exhibit two characteristic bands [30; 31; 34]. One is the band at $\nu = 1580$ $cm^{-1}$, allowed by Raman scattering and corresponding to the ideal graphitic vibrational mode with $E_{2g}$ symmetry, often referred to as the *G* mode [23–27]. It is associated with in-plane vibrations of carbon atoms in graphene layers and relates to carbon atoms in an $sp^2$-hybridized state. The other band, at $\nu = 1360$ $cm^{-1}$, is due to disordered carbon atoms, corresponds to lattice vibrations with $A_{1g}$ symmetry, and is called the *D* mode [23–27]. This mode is linked to carbon atoms in $sp^2$- and $sp^3$ hybridization states, typically localized at defects or the edges of graphene layers [23–27]. The *D* band is absent in monocrystalline graphite, and its increasing intensity is considered indicative of a higher content of disordered or peripheral carbon [23–27]. According to numerous studies, for crystallite sizes up to 2 nm, the ratio of the integrated intensities of these bands ($I_D/I_G$) depends on the defect concentration and follows the Ferrari equation [28; 30–32]. For crystallite sizes larger than 2 nm, the $I_D/I_G$ ratio is determined by the average distance between defects. In graphitizing carbon materials, it can characterize the average crystallite size ($L_a$) using the Tuinstra-Koenig relation [29–31]. For the studied CF, $L_a$ was calculated using the following equation:

$$\frac{I_D}{I_G} = \frac{C(\lambda)}{L_a}, \quad (1)$$

where $C(\lambda)$ is a constant dependent on the laser wavelength. Thus, $C(\lambda = 532\ nm)$ is approximately equal to 4.4 nm [23; 24; 27].

The interpretation of the secondary 2*D* band ($\nu = 2700$ $cm^{-1}$) is more complex. This band appears at a sufficiently high degree of crystalline structure perfection and typically consists of several components [24; 27]. However, for the purposes of this study, only the $t_{HT}$ (heat-treatment temperature) at which the 2*D* band appears was recorded.

*X*-ray phase analysis was conducted using a D8 Advance diffractometer (Bruker, Germany). A copper *X*-ray tube with a maximum power of 2200 *W* and Cu$K_\alpha$ radiation ($\lambda = 0.15418$ nm) was used as the *X*-ray source, in Bragg–Brentano geometry (reflection mode). *X*-ray diffraction patterns were recorded over the angular range of $2\theta = 10 \div 90°$, with a scanning speed of 2°/min and a step size of 0.02°. The fibers were placed on a low-background silicon holder, evenly distributed over its surface. Before each measurement, the tube and detector were initialized. The diffraction patterns were processed using the specialized TOPAS software. The absolute error in measuring the angular positions of diffraction peaks did not exceed ±0.026° [33]. The interplanar spacing ($d_{002}$) was calculated based on the center of gravity of the (002) peak using the Wulff–Bragg equation:

$$d_{002} = \frac{\lambda}{2\sin\theta_{002}}, \quad (2)$$

where λ is the wavelength of the *X*-ray radiation and $\theta_{002}$ is the diffraction angle determined from the center of gravity of the (002) reflection.

The crystallite sizes were calculated using the Scherrer formula:

$$L_c = \frac{k\lambda}{\beta\cos\theta_{002}}, \quad (3)$$

where β is the full width at half maximum (FWHM) of the (002) reflection, and $k = 0.89$ [32; 33].

## Results and discussion

Fig. 1 presents photographs of PAN- and viscose-based CF filaments treated at processing temperatures $t_{HT}$ = 1200 and 2800 °C. It is evident that the microstructure of the fracture surface and the lateral surface of the filaments of the studied CF at $t_{HT}$ = 1200 °C show minimal differences. However, the fracture surface photographs of the CF after heat treatment at 2800 °C exhibit pronounced differences.

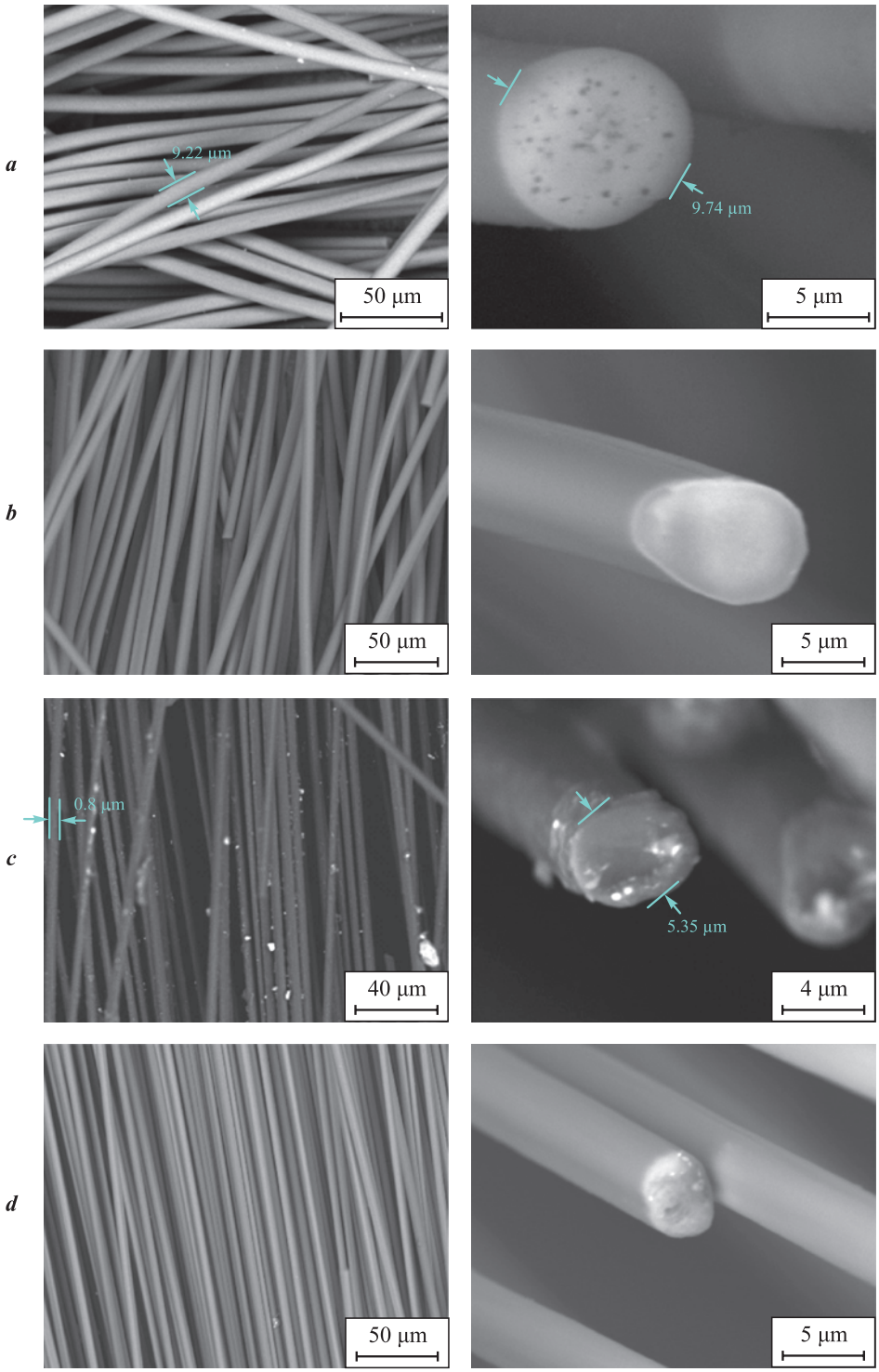


***Fig. 1.*** Photographs of viscose-based CF (***a***, ***b***) and PAN-based CF filaments (***c***, ***d***) at $t_{HT}$ = 1200 °C (***a***, ***c***) and 2800 °C (***b***, ***d***)

***Рис. 1.*** Фотографии филаментов УВ на основе вискозы (***a***, ***b***) и ПАН (***c***, ***d***) $t_{ТО}$ = 1200 °C (***a***, ***c***) и 2800 °C (***b***, ***d***)

The dependencies of the true density of CF filaments (γ, g/cm$^3$) and the dynamic elastic modulus ($E$, GPa) on the processing temperature of the studied fibers are shown in Fig. 2. It can be seen that viscose-based fibers exhibit lower values of γ and $E$ compared to PAN-based CF across the entire range of $t_{HT}$. Notably, the elastic modulus of viscose-based fibers is 4–5 times lower than that of PAN-based fibers throughout the temperature range.

Fig. 3 shows the $X$-ray diffraction patterns and Raman spectra of the studied CF with varying processing temperatures, while Fig. 4 illustrates the dependence of their crystalline structure parameters on $t_{HT}$.

It is evident that the increase in intensity and narrowing of the (002) diffraction line indicates an improvement in the crystalline structure with increasing $t_{HT}$ for both viscose- and PAN-based CF (Fig. 3, *a*, *b*). The asymmetry of the diffraction peak can be effectively described by multiple structural components [34–35]; however, this study provides averaged data for one of these components.

In the Raman spectra of the studied CF (Fig. 3, *c*, *d*), the $D$ and $G$ bands become narrower with increasing $t_{HT}$, and the relative intensity of the $D$ peak decreases. After heat treatment at $t \sim 1800$ °C, the 2$D$ peak appears, and its intensity relative to the $G$ peak increases with rising processing temperature.

However, after heat treatment at 2800 °C, the differences in the crystalline structure parameters of viscose- and PAN-based CF become insignificant or disappear entirely (see Fig. 3), except for the crystallite size $L_a$ (see Fig. 4).

Fig. 5 shows the dependencies of Raman spectroscopy parameters for viscose-based CFs (*1*) and PAN-based CFs (*2*) on the processing temperature.

It is evident that the positions and widths of the $D$ and $G$ bands systematically change with increasing $t_{HT}$. In accordance with the results of previous studies, the dependence of the $I_D/I_G$ parameter was previously used by us to evaluate the effective processing temperature of PAN-based CFs [36].

Using a similar approach, empirical expressions for determining the effective processing temperature ($t_{eff}$, °C) of PAN-based (4) and viscose-based (5) CFs were derived based on the obtained dependencies of the $I_D/I_G$ parameter on $t_{HT}$ (see Fig. 5, *a*):

$$t_{eff} = 2089 - \left(901 \ln \frac{I_D}{I_G}\right), \quad (4)$$

$$t_{eff} = 1815 - \left(641 \ln \frac{I_D}{I_G}\right). \quad (5)$$

## Conclusion

The results of the study indicate that viscose-based carbon fibers (CFs) exhibit a significantly lower degree of crystalline structure perfection compared to PAN-based CFs across almost the entire range of heat treatment temperatures. However, high-temperature treatment at 2800 °C largely mitigates these differences, suggesting partial graphitization of viscose-based CFs. Nevertheless, as evidenced by the full set of obtained data, despite the similarity in most crystalline structure parameters, viscose-based CFs do not

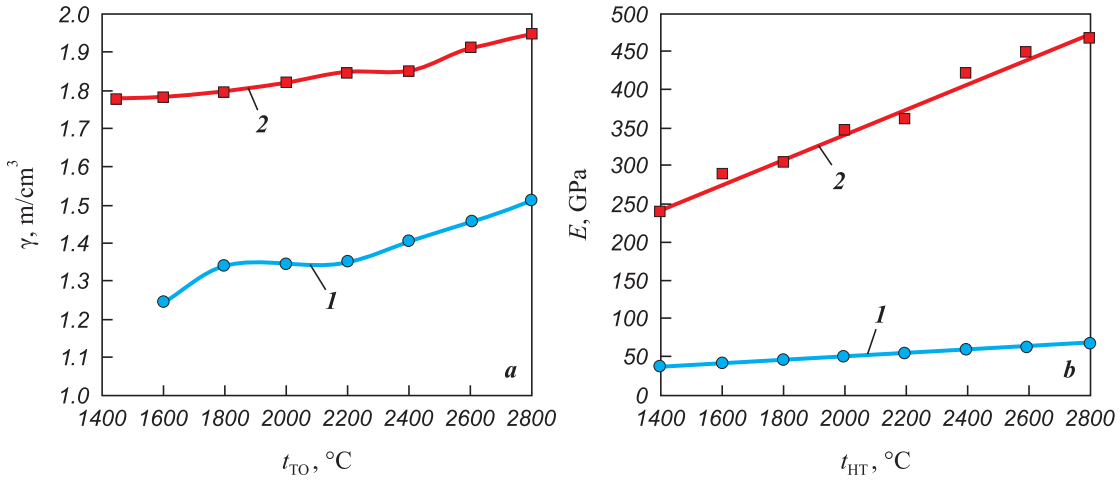


***Fig. 2.*** Dependence of true density (***a***) and dynamic elastic modulus (***b***) on the processing temperature for viscose-based (***1***) and PAN-based (***2***) carbon fibers

***Рис. 2.*** Зависимость истинной плотности (***a***) и динамического модуля упругости (***b***) от температуры обработки УВ на основе вискозы (***1***) и ПАН (***2***)

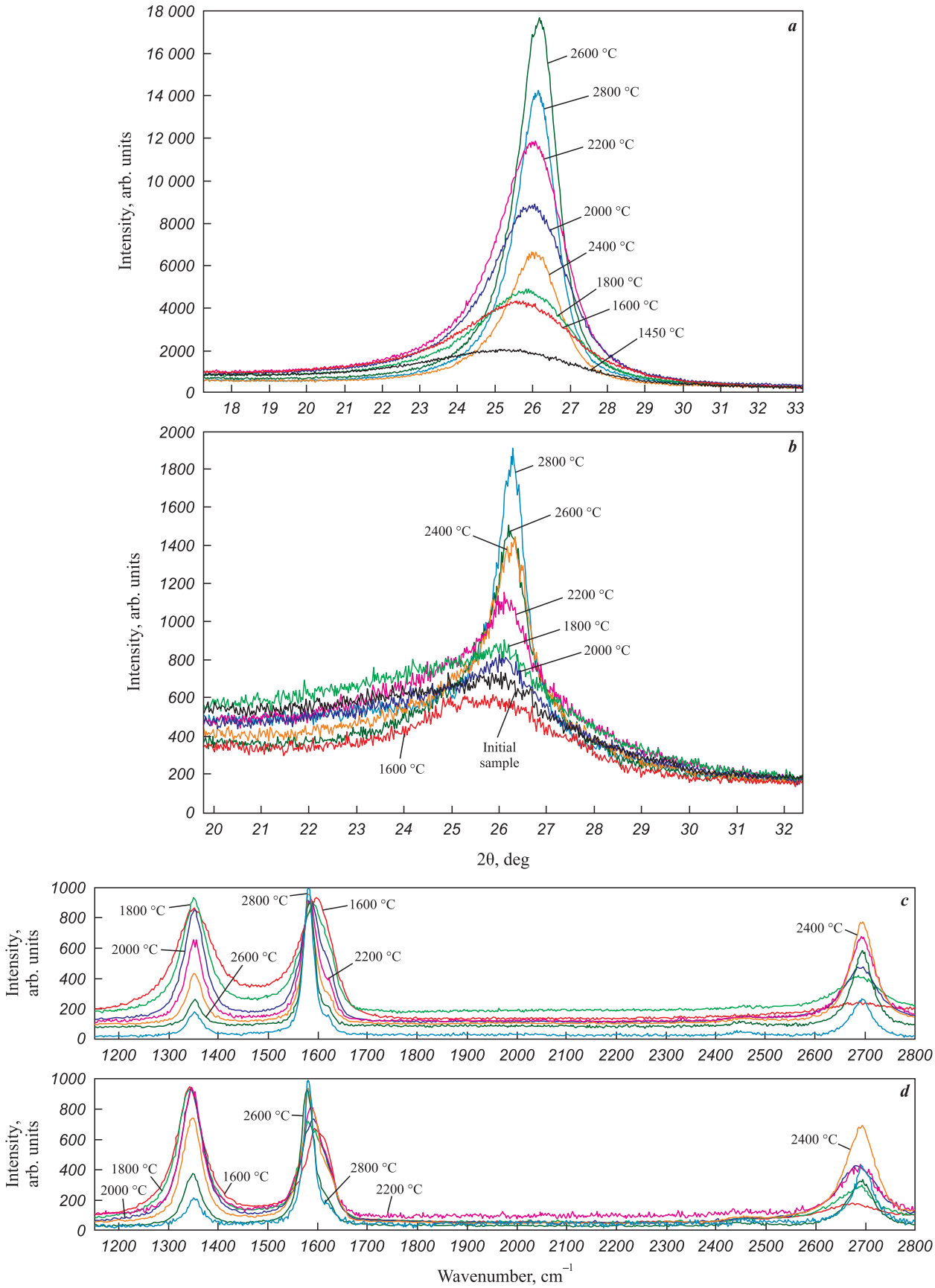


***Fig. 3.*** *X*-ray diffraction patterns of CFs (***a***, ***b***) based on PAN (***a***), and viscose (***b***), and Raman spectra of CFs (***c***, ***d***) based on PAN (***c***), and viscose (***d***)

***Рис. 3.*** Рентгенограммы (***a***, ***b***) и спектры комбинационного рассеяния (***c***, ***d***) УВ на основе ПАН (***a***, ***c***) и вискозы (***b***, ***d***)

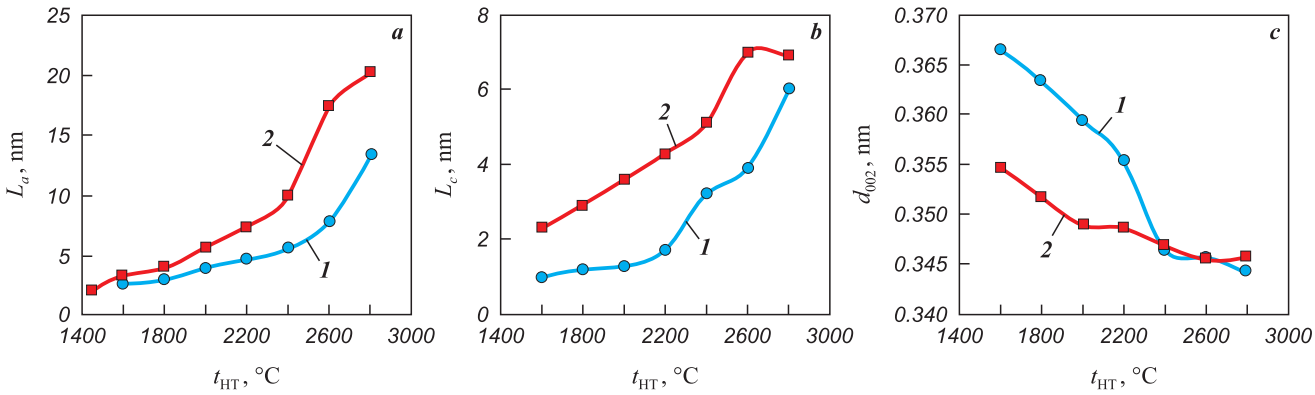


***Fig. 4.*** Dependence of crystalline structure parameters on the processing temperature of fibers based on viscose (***1***) and PAN (***2***)
***a*** – crystallite size $L_a$; ***b*** – crystallite sizes $L_c$; ***c*** – interlayer spacing $d_{002}$

***Рис. 4.*** Температурные зависимости параметров кристаллической структуры волокон на основе вискозы (***1***) и ПАН (***2***)
***a*** – размеры кристаллитов $L_a$; ***b*** – размеры кристаллитов $L_c$; ***c*** – межслоевое расстояние $d_{002}$

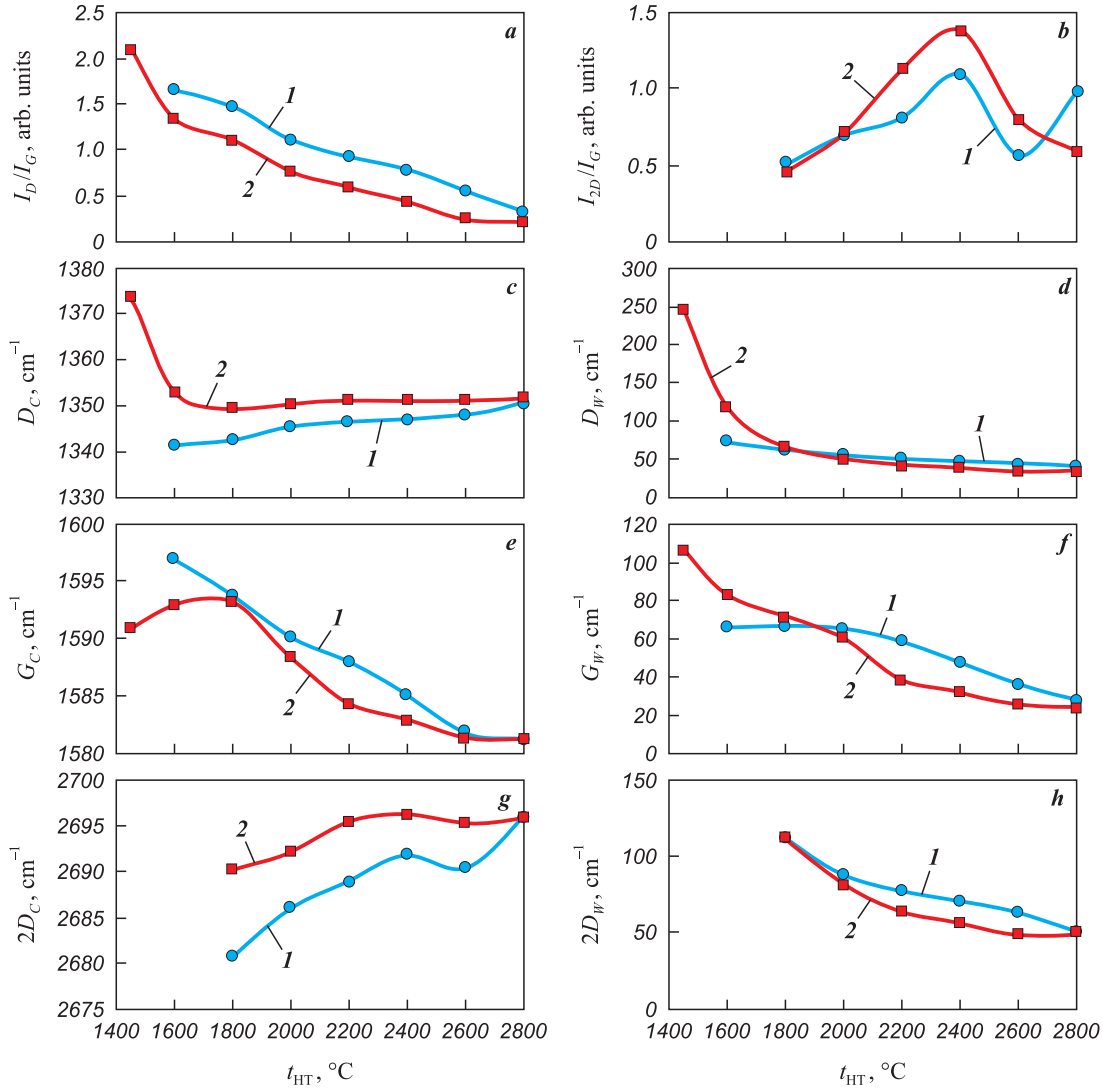


***Fig. 5.*** Dependence of Raman spectroscopy parameters for viscose-based CFs (***1***) and PAN-based CFs (***2***) on the heat treatment temperature

***Рис. 5.*** Зависимости параметров рамановской спектроскопии для УВ на основе вискозы (***1***) и ПАН (***2***) от температуры термообработки

become equivalent to PAN-based CFs even after high-temperature treatment. The elastic modulus of viscose-based CFs does not exceed 100 GPa, which is over four times lower the elastic modulus of PAN-based CFs subjected to identical treatment conditions. The true density of viscose-based CFs remains significantly lower compared to PAN-based CFs (see Fig. 2, *a*), indicating the distinctive nature of their porosity.

These differences, in our view, can be attributed to the inherently low degree of microtexturing in viscose-based CFs compared to PAN-based CFs and, to an even greater extent, to mesophase pitch-based CFs [19; 37]. The closest counterpart to low-modulus viscose-based CFs are fibers produced from isotropic pitches [10], which similarly exhibit reduced true density and microtexturing.

Based on previous studies [7; 22], which found no significant differences in the properties of the raw viscose fibers used for CF production, it can be inferred that the low elastic modulus of the investigated viscose-based CFs is primarily due to the absence of intensive orientational stretching during the graphitization process.

## References / Список литературы

1. Gupta M.K., Singhal V., Rajput N.S. Applications and challenges of carbon-fibres reinforced composites: A review. *Evengreen Joint Journal of Novel Carbon Resource Sciences & Green Asia Strategy*. 2022;9(3):682–693. https://doi.org/10.5109/4843099
2. Ince J.C., Peerzada M., Mathews L.D., Pai A.R., Alqatatsheh A., Abbasi S., Yin Y., Hameed N., Duffy A.R., Lau A.K., Salim N.V. Overview of emerging hybrid and composite materials for space applications. *Advanced Composites and Hybrid Materials*. 2023;6(4):130. https://doi.org/10.1007/s42114-023-00678-5
3. Zhao J. Carbon fiber applications in modern rockets. *Preprint*. June 2023. https://doi.org/10.13140/RG.2.2.12957.49126
4. Olofin I., Liu R. The application of carbon fibre reinforced polymer (CFRP) cables in civil engineering structures. *International Journal of Civil Engineering*. 2015;2(7):1–5. https://doi.org/10.14445/23488352/IJCE-V2I7P101
5. Ozkan D., Gok M.S., Karaoglanli A.C. Carbon fiber reinforced polymer (CFRP) composite materials, their characteristic properties, industrial application areas and their machinability. In: *Öchsner A., Altenbach H. (eds). Engineering Design Applications III. Advanced Structured Materials, vol. 124*. Springer, Cham. 2020. P. 235–253. https://doi.org/10.1007/978-3-030-39062-4_20
6. Morgan P. Carbon fibers and their composites. London: Taylor & Francis Group, 2005. 1166 p. https://doi.org/10.1201/9781420028744
7. Park S.-J., Heo G.-Y. Precursors and manufacturing of carbon fibers. In: *Carbon Fibers. Springer Series in Materials Science, vol. 210*. Springer, Dordrecht. 2014. P. 31–66. https://doi.org/10.1007/978-94-017-9478-7_2
8. Emmerich F.G. Young's modulus, thermal conductivity, electrical resistivity and coefficient of thermal expansion of mesophase pitch-basedcarbonfibers. *Carbon*. 2014;79:274–293. https://doi.org/10.1016/j.carbon.2014.07.068
9. Frank E., Steudle L.M., Ingildeev D., Spörl J.M., Buchmeiser M.R. Carbon fibers: Precursor systems, processing, structure, and properties. *Angewandte Chemie International Edition*. 2014;53(21):5262–5298. https://doi.org/10.1002/anie.201306129
10. Newcomb B.A. Processing, structure, and properties of carbon. *Composites Part A: Applied Science and Manufacturing*. 2016;91:262–282. https://doi.org/10.1016/j.compositesa.2016.10.018
11. Mirdehghan S.A. Fibrous polymeric composites. In: *Engineered polymeric fibrous materials. The Textile Institute. Book Series*. Woodhead Publishing, 2021. P. 1–58. https://doi.org/10.1016/B978-0-12-824381-7.00012-3
12. Qiu L., Zheng X.H., Zhu J., Su G.P., Tang D.W. The effect of grain size on the lattice thermal conductivity of an individual polyacrylonitrile-based carbon fiber. *Carbon*. 2013;51:265–273. https://doi.org/10.1016/j.carbon.2012.08.052
13. Sun Z., Lu Y., Wang R., Yang C. Analysis of carbon fiber structure based on dynamic laser Raman spectroscopy. *Journal of Applied Polymer Science*. 2020;138(16):50247. https://doi.org/10.1002/app.50247
14. Li D., Wang H., Wang X. Effect of microstructure on the modulus of PAN-based carbon fibers during high temperature treatment and hot stretching graphitization. *Journal of Materials Science*. 2007;42(12):4642–4649. https://doi.org/10.1007/s10853-006-0519-4
15. Zhou G., Liu Y., He L., Guo Q., Ye H. Microstructure difference between core and skin of T700 carbon fibers in heat-treated carbon/carbon composites. *Carbon*. 2011;49(9):2883–2892. https://doi.org/10.1016/j.carbon.2011.02.025
16. Wu G.-P., Li D.-H., Yang Y., Lu C.-X., Zhang S.-C., Li X.-T., Feng Z.-H., Li Z.-H. Carbon layer structures and thermal conductivity of graphitized carbon fibers. *Journal of Materials Science*. 2011;47(6):2882–2890. https://doi.org/10.1007/s10853-011-6118-z
17. Qin X., Lu Y., Xiao H., Wen Y., Yu T. A comparison of the effect of graphitization on microstructures and properties of polyacrylonitrile and mesophase pitch-based carbon fibers. *Carbon*. 2012;50(12):4459–4469. https://doi.org/10.1016/j.carbon.2012.05.024
18. Sarian S., Strong S.L. Mechanical properties of stress-graphitised carbon fibers: Thermally induced relaxation and recovery. *Fibre Science and Technology*. 1971;4(1):67–79. https://doi.org/10.1016/0015-0568(71)90012-1
19. Diefendorf R.J., Tokarsky E. High-performance carbon fibers. *Polymer Engineering and Science*. 1975;15(3): 150–159. https://doi.org/10.1002/pen.760150306
20. Spörl J. M., Ota A., Son S., Massonne K., Hermanutz F., Buchmeiser M.R. Carbon fibers prepared from ionic liquid-derived cellulose precursors. *Materials Today Com-*

*munications*. 2016;7:1–10.
https://doi.org/10.1016/j.mtcomm.2016.02.002

**21.** Bengtsson A., Bengtsson J., Sedin M., Sjöholm E. Carbon fibres from lignin-cellulose precursors: Effect of stabilisation conditions. *ACS Sustainable Chemistry & Engineering*. 2019;7(9):8440–8448.
https://doi.org/10.1021/acssuschemeng.9b00108

**22.** Dumanli A.G., Windle A.H. Carbon fibres from cellulosic precursors: A review. *Journal of Materials Science*. 2012;47(10):4236–4250.
https://doi.org/10.1007/s10853-011-6081-8

**23.** Tuinstra F., Koenig J.L. Raman spectrum of graphite. *The Journal of Chemical Physics*. 1970;53(3):1126–1130.
https://doi.org/10.1063/1.1674108

**24.** Cançado L.G., Takai K., Enoki T., Endo M., Kim Y.A., Mizusaki H., Jorio A., Coelho L.N., Magalhães Paniago R., Pimenta M.A. General equation for the determination of the crystallite size $L_a$ of nanographite by Raman spectroscopy. *Applied Physics Letters*. 2006;88(16):3106–3109.
https://doi.org/10.1063/1.2196057

**25.** Reich S., Thomsen C. Raman spectroscopy of graphite. *Philosophical Transactions of the Royal Society A: Mathematical, Physical and Engineering Sciences*. 2004; 362(1824):2271–2288.
https://doi.org/10.1098/rsta.2004.1454

**26.** Ferrari A.C., Robertson J. Interpretation of Raman spectra of disordered and amorphous carbon. *Physical Review B*. 2000;61(20):14095–14107.
https://doi.org/10.1103/physrevb.61.14095

**27.** Cancado L.G., Jorio A., Martins Ferreira E.H., Stavale F., Achete C.A., Capaz R.B., Moutinho M.V.O., Lombardo A., Kulmala T.S., Ferrari A.C. Quantifying defects in graphene via Raman spectroscopy at different excitation energies. *Nano Letters*. 2011;11(8):3190–3196.
https://doi.org/10.1021/nl201432g

**28.** Ferrari A.C., Basko D.M. Raman spectroscopy as a versatile tool for studying the properties of graphene. *Nature Nanotechnology*. 2013;8(4):235–246.
https://doi.org/10.1038/nnano.2013.46

**29.** Zickler Gerald A., Smarsly B., Gierlinger N., Peterlik H., Paris O.A reconsideration of the relationship between the crystallite size $L_a$ of carbons determined by *X*-ray diffraction and Raman spectroscopy. *Carbon*. 2006;44(15): 3239−3246.
https://doi.org/10.1016/j.carbon.2006.06.029

**30.** Okuda H., Young R. J., Wolverson D., Tanaka F., Yamamoto G., Okabe T. Investigating nanostructures in carbon fibres using Raman spectroscopy. *Carbon*. 2018; 130:178–184.
https://doi.org/10.1016/j.carbon.2017.12.108

**31.** Samoilov V.M., Samsonova V.B., Nakhodnova A.V., Verbets D.B., Gareev A.R., Bubnenkov I.A., Steparyova N.N., Shvetsov A.A., Bardin N.G. Raman spectroscopy and crystalline structure of polyacrylonitrile-based carbon fibres. *Advanced Materials & Technologies*. 2019;3(15):8–15.
https://doi.org/10.17277/amt.2019.03.pp.008-015

**32.** Pacault A. Chemistry and physics of carbon. Ed. L. Walker. Vol. 7. N.Y.: Marcel Dekker, 1971. 403 p.

**33.** Cheblakova E.G. , Kleusov B.S., Sapozhnikov V.I. , Gorina V.A., Malinina Yu.A., Gareev A.R. Investigation of the properties of high-strength fibers by methods of physico-chemical analysis. *Powder Metallurgy and Functional Coatings*. 2023;17(4):34–40.
https://doi.org/10.17073/1997-308X-2023-4-34-40

Чеблакова Е.Г., Клеусов Б.С., Сапожников В.И., Горина В.А., Малинина Ю.А., Гареев А.Р. Исследования свойств высокопрочных волокон методами физико-химического анализа. *Известия вузов. Порошковая металлургия и функциональные покрытия*. 2023;17(4):34–40.
https://doi.org/10.17073/1997-308X-2023-4-34-40

**34.** Tyumentsev V.A., Fazlitdinova A.G., Podkopaev S.A., Churikov V.V. Fine structure of polyacrylonitrile and carbon fibers. *Izvestiya vuzov. Khimiya i khimicheskaya tekhnologiya*. 2013;56(7):83–87. (In Russ.).

Тюменцев В.А., Фазлитдинова А.Г., Подкопаев С.А., Чуриков В.В. Тонкая структура полиакрилонитрильных и углеродных волокон. *Известия вузов. Химия и химическая технология*. 2013;56(7):83–87.

**35.** Tyumentsev V.A., Fazlitdinova A.G. Study of the structure of fibrous carbon materials by *X*-ray diffractometry. *Zavodskaya laboratoriya. Diagnostika materialov*. 2019; 85(11):31–36. (In Russ.).
https://doi.org/10.26896/1028-6861-2019-85-11-31-36

Тюменцев В.А., Фазлитдинова А.Г. Исследование структуры волокнистых углеродных материалов методом рентгеновской дифрактометрии. *Заводская лаборатория. Диагностика материалов*. 2019; 85(11):31–36.
https://doi.org/10.26896/1028-6861-2019-85-11-31-36

**36.** Samoilov V.M., Nakhodnova A.V., Osmova M.A., Verbets D.B., Bubnenkov A.N., Steparyova N.N., Gareev A.R., Fateeva M.A., Shilo D.V., Ovsyannikov N.E. Effective heat treatment temperature of carbon materials in high temperature furnaces: determination by the parameters of raman spectroscopy of witness samples. *Inorganic Materials: Applied Research*. 2021;12(5):1416–1427.
https://doi.org/10.1134/S2075113321050348

Самойлов В.М., Находнова А.В., Осмова М.А., Вербец Д.Б., Бубненков А.Н., Степарева Н.Н., Гареев А.Р., Фатеева М.А., Шило Д.В., Овсянников Н.Е. Определение эффективной температуры обработки углеродных материалов в высокотемпературных печах по параметрам спектроскопии комбинационного рассеяния образцов-свидетелей. *Перспективные материалы*. 2021;1:67–84.
https://doi.org/10.30791/1028-978X-2021-1-67-84

**37.** Northolt M.G., Veldhuizen L.H., Jansen H. Tensile deformation of carbon fibers and the relationship with the modulus for shear between the basal planes. *Carbon*. 1991;29(8):1267–1279.
https://doi.org/10.1016/0008-6223(91)90046-l

## Information about the Authors

***Boris S. Kleusov*** – Senior Researcher, Testing Center, Joint Stock Company "Scientific Research Institute of Structural Materials Based on Graphite named after S.E. Vyatkin" (JSC "NIIgrafit")
***ORCID***: 0000-0003-3924-2616
***E-mail:*** BSKleusov@rosatom.ru

***Vladimir M. Samoilov*** – Chief Researcher, JSC "NIIgrafit"
***ORCID***: 0000-0002-9861-905X
***E-mail:*** vmsamoylov@rosatom.ru

***Victoria A. Elchavinova*** – Researcher, JSC "NIIgrafit"
***ORCID***: 0009-0006-3167-8924
***E-mail:*** Viaelchaninova@rosatom.ru

***Dmitry A. Budushin*** – Intern Researcher, JSC "NIIgrafit"
***ORCID***: 0009-0002-4239-1145
***E-mail:*** DABudushin@rosatom.ru

***Egor M. Litovchenko*** – Student, D.I. Mendeleev Russian University of Chemical Technology
***ORCID***: 0009-0001-3381-855X
***E-mail:*** litovtch.egor@yandex.ru

***Anna S. Poplavskaya*** – Engineer, JSC "NIIgrafit"
***ORCID***: 0009-0004-0028-9411
***E-mail:*** ASPoplavskaya@rosatom.ru

***Vladimir A. Vorontsov*** – Department Head, JSC "NIIgrafit"
***ORCID***: 0009-0004-2684-1665
***E-mail:*** VlAVorontsov@rosatom.ru

## Сведения об авторах

***Борис Сергеевич Клеусов*** – ст. науч. сотрудник Испытательного центра АО «Научно-исследовательский институт конструкционных материалов на основе графита им. С.Е. Вяткина» (АО «НИИграфит»)
***ORCID***: 0000-0003-3924-2616
***E-mail:*** BSKleusov@rosatom.ru

***Владимир Маркович Самойлов*** – гл. науч. сотрудник АО «НИИграфит»
***ORCID***: 0000-0002-9861-905X
***E-mail:*** vmsamoylov@rosatom.ru

***Виктория Андреевна Ельчанинова*** – науч. сотрудник АО «НИИграфит»
***ORCID***: 0009-0006-3167-8924
***E-mail:*** Viaelchaninova@rosatom.ru

***Дмитрий Алексеевич Будушин*** – стажер-исследователь АО «НИИграфит»
***ORCID***: 0009-0002-4239-1145
***E-mail:*** DABudushin@rosatom.ru

***Егор Максимович Литовченко*** – студент Российского химико-технологического университета им. Д.И. Менделеева
***ORCID***: 0009-0001-3381-855X
***E-mail:*** litovtch.egor@yandex.ru

***Анна Сергеевна Поплавская*** – инженер АО «НИИграфит»
***ORCID***: 0009-0004-0028-9411
***E-mail:*** ASPoplavskaya@rosatom.ru

***Владимир Алексеевич Воронцов*** – руководитель направления АО «НИИграфит»
***ORCID***: 0009-0004-2684-1665
***E-mail:*** VlAVorontsov@rosatom.ru

## Contribution of the Authors

***B. S. Kleusov*** – performed *X*-ray phase analysis and participated in the discussion of results.
***V. M. Samoilov*** – conducted data analysis and participated in the discussion of results.
***V. A. Elchaninova*** – conducted Raman spectroscopy.
***D. A. Budushin*** – performed data analysis and prepared for the article.
***E. M. Litovchenko*** – prepared figures for the article and participated in the discussion of data.
***A. S. Poplavskaya*** – conducted scanning electron microscopy.
***V. A. Vorontsov*** – measured the dynamic elastic modulus.

## Вклад авторов

***Б. С. Клеусов*** – проведение рентгенофазового анализа, участие в обсуждении результатов.
***В. М. Самойлов*** – анализ данных, участие в обсуждении результатов.
***В. А. Ельчанинова*** – проведение рамановской спектроскопии.
***Д. А. Будушин*** – проведение анализа и подготовка данных для статьи.
***Е. М. Литовченко*** – создание иллюстраций, участие в обсуждении данных.
***А. С. Поплавская*** – проведение сканирующей электронной микроскопии.
***В. А. Воронцов*** – измерение динамического модуля упругости.

Received 16.08.2024
Revised 25.10.2024
Accepted 28.10.2024

Статья поступила 16.08.2024 г.
Доработана 25.10.2024 г.
Принята к публикации 28.10.2024 г.